Response of Planetary Waves to Stationary Tropical Heating in a Global Atmosphere with Meridional and Vertical Shear

AKIRA KASAHARA

National Center for Atmospheric Research, Boulder, CO 80307*

PEDRO L. DA SILVA DIAS

Department of Meteorology, Institute of Astronomy and Geophysics, University of São Paulo, 01000–São Paulo, Brazil

(Manuscript received 14 October 1985, in final form 7 March 1986)

ABSTRACT

The response of planetary waves to stationary tropical heating in a stratified global atmosphere linearized with respect to a basic zonal mean flow is investigated. The basic zonal wind has meridional and vertical shear. The basic equations are solved by using the method of three-dimensional normal-mode expansion. Forced solutions to a prescribed tropospheric equatorial heating distribution with a specific wavenumber in longitude are examined.

Without the basic zonal flow, the internal vertical modes whose equivalent depths are on the order of a few hundred meters are favorably excited, but the response of the external mode ("barotropic" mode) is relatively small. With the inclusion of a zonal flow, the vertical shear of the zonal wind permits the coupling of the external mode with the internal vertical modes. As a result of the coupling, a significant response occurs in the external mode due to the excitation of the "baroclinic" internal modes by tropical heating. The meridional structures of internal vertical modes are equatorially trapped and their intensities are less affected by the basic zonal flow. Since the meridional structures of the external mode is global, a significant response of the external mode to tropospheric tropical heating is no longer confined to the tropics. The direction of the basic zonal flow and its meridional shear have a profound influence on the intensity of planetary waves in the mid- to higher latitudes generated by stationary tropical heating. The present findings may fill in a missing link in the dynamical theory of atmospheric teleconnections.

1. Introduction

In an earlier work (Kasahara, 1984, hereafter referred to as K84), the linear response of a stratified global atmosphere to tropical heating was investigated by using a normal mode expansion in both the vertical and horizontal directions. It was shown that the vertical internal modes whose vertical profiles have "baroclinic" structures are favorably excited by tropical heating in agreement with Geisler and Stevens (1982), Lim and Chang (1983) and Fulton and Schubert (1985). Moreover, the appearance of an anticyclonic pair in the upper troposphere sitting astride the equatorial heat source agrees with many related studies (e.g., Matsuno, 1966; Gill, 1980; Geisler, 1981; Moura and Shulka, 1981; Lim and Chang, 1981; Lau and Lim, 1982; Silva Dias et al., 1983). One notable finding in K84 was that the response of the external mode is relatively small, though it is by no means negligible. Since the largest portion of atmospheric energy is observed to reside in the external mode, the question may be raised whether or not the dominance of the internal modes, corresponding to the equivalent heights of a few hundred meters, is inconsistent with observation.

This question may be partly resolved by considering the fact that the K84 study did not take into account the effects of the basic zonal flow. Aiming at the study of steady, linear response of a stratified atmosphere to tropical thermal forcing, Webster (1972) used a two-level linearized primitive-equation global model and calculated the dynamical response of the model atmosphere, in which the basic zonal flow has both meridional and vertical shear, to tropical forcings. Later, Webster (1981, 1982) made extensive numerical calculations with essentially the same model configuration to investigate the mechanisms by which sea surface temperature anomalies give rise to atmospheric responses and to study the seasonal variation of the atmospheric response to tropical heating. It is clear from these studies, and also from Opsteegh and Van den Dool (1980), that the response to tropical heating appears not only in the vicinity of the heat source, but also in the middle to higher latitudes. Moreover, the basic zonal flow plays an important role in determining

* The National Center for Atmospheric Research is sponsored by the National Science Foundation.

the extent of middle to higher latitude response to tropical thermal forcings.

Detailed analyses of the three-dimensional aspect of the response of a global atmosphere to prescribed forcings were also made by Hoskins and Karoly (1981), Hendon and Hartmann (1982), Simmons (1982) and Rosenlof et al. (1986) using linear, steady, multilayered baroclinic models. One notable finding from these studies is that the responses to tropical heating are baroclinic in character in the vicinity of the heat sources, while the responses become equivalent barotropic away from the forcing regions. In fact, the middle to higher latitude responses are very similar to those induced by tropical forcings in a barotropic atmosphere (Hoskins et al., 1977). There is little doubt that once the tropical forcings have excited equivalent barotropic disturbances, then they will propagate away from the source regions. The basic zonal flow in the linearized models must play an important role in meridional energy propagation as envisaged by Charney (1969). However, we must still answer the question by what mechanism are equivalent barotropic disturbances generated in the first place by tropospheric tropical forcings. Lim and Chang (1983) have suggested that the vertical shear of mean zonal wind plays an important role in this respect.

The purpose of this paper is to investigate the effects of basic mean zonal flow in calculating the steady response of a linearized global atmosphere to tropical heating. The basic mean zonal flow has meridional and vertical shear. The basic equations are presented in section 2, and steady state solutions to a prescribed heating distribution are discussed in section 3. For the basic mean zonal flow, we assume a constant vertical shear with a climatological zonal wind at the 500 mb level. Numerical results of steady responses to a prescribed equatorial heating in the model with and without the vertical shear of zonal flow are presented in section 4. We will show that the presence of vertical zonal-wind shear permits the coupling of the external vertical mode with the internal vertical modes and a significant response occurs in the external mode as a result of exciting the "baroclinic" internal modes due to tropical heating. The meridional structures of higher internal modes are equatorially trapped and their intensities are less affected by the basic zonal flow. Since the meridional structure of the external mode is global, the contribution of this mode in addition to the internal modes produces a significant global response to tropical heating. The direction of the basic zonal flow and its meridional shear have a profound influence on the intensity of planetary waves in the mid- to higher latitudes generated by stationary tropical heating, as discussed in section 5. The present finding will be useful in interpreting the planetary wave response in the middle to higher latitudes to tropical heating anomalies simulated in general circulation models, as further discussed in section 6.

2. Basic equations

We adopt spherical coordinates of longitude λ and latitude ϕ, increasing eastward and northward, respectively, and modified pressure coordinates σ, defined by

$$\sigma = 2p/p_s - 1, \tag{2.1}$$

where p and p_s denote the pressure and a constant pressure near the earth's surface, respectively.

Zonal and meridional velocity components u and v, vertical σ velocity ω ($\equiv d\sigma/dt$), temperature T, and isobaric height z are expressed by

$$\left.\begin{aligned} u &= \bar{u}(\phi,\sigma) + u'(\lambda,\phi,\sigma,t) \\ v &= v'(\lambda,\phi,\sigma,t) \\ \omega &= \omega'(\lambda,\phi,\sigma,t) \\ T &= T_0(\sigma) + \bar{T}(\phi,\sigma) + T'(\lambda,\phi,\sigma,t) \\ z &= z_0(\sigma) + \bar{z}(\phi,\sigma) + z'(\lambda,\phi,\sigma,t) \end{aligned}\right\}, \tag{2.2}$$

where t denotes time.

In (2.2), $T_0(\sigma)$ and $z_0(\sigma)$ represent the standard atmospheric temperature distribution and the corresponding isobaric height distribution. They satisfy the hydrostatic equation

$$g\frac{dz_0}{d\sigma} = -\frac{RT_0}{1+\sigma} \tag{2.3}$$

with g and R denoting, respectively, the earth's gravitational acceleration and the specific gas constant. Also, $\bar{u}$, $\bar{T}$ and $\bar{z}$ represent the basic zonal flow and are related by the hydrostatic equation

$$g\frac{\partial \bar{z}}{\partial \sigma} = -\frac{R\bar{T}}{1+\sigma} \tag{2.4}$$

and a gradient wind equation

$$\left(2\Omega \sin\phi + \frac{\bar{u}}{a}\tan\phi\right)\bar{u} + \frac{g\partial \bar{z}}{a\partial\phi} = 0, \tag{2.5}$$

with Ω and a denoting, respectively, the earth's angular velocity and radius, which are treated as constants. In (2.2), u', v', ω', T' and z' are perturbation quantities representing the deviations from the standard atmosphere and the basic zonal flow.

We write the system of linearized equations utilizing the equations of horizontal motion, continuity and thermodynamics

$$\left.\begin{aligned} &\frac{\partial u'}{\partial t} - 2\Omega \sin\phi v' + \frac{g}{a\cos\phi}\frac{\partial z'}{\partial \lambda} = C_1 \\ &\frac{\partial v'}{\partial t} + 2\Omega \sin\phi u' + \frac{g}{a}\frac{\partial z'}{\partial \phi} = C_2 \\ &\frac{\partial}{\partial t}\left\{-\frac{\partial}{\partial \sigma}\left[\frac{g(1+\sigma)}{R\Gamma_0}\frac{\partial z'}{\partial \sigma}\right]\right\} + \nabla\cdot\mathbf{V}' = \frac{\partial C_3}{\partial \sigma} \end{aligned}\right\}, \tag{2.6}$$

where

$$\left.\begin{aligned} C_1 &= -\frac{\bar{u}}{a\cos\phi}\frac{\partial u'}{\partial\lambda} - \frac{v'}{a}\frac{\partial\bar{u}}{\partial\phi} - \omega'\frac{\partial\bar{u}}{\partial\sigma} + \frac{\bar{u}v'\tan\phi}{a} + F_\lambda \\ C_2 &= -\frac{\bar{u}}{a\cos\phi}\frac{\partial v'}{\partial\lambda} - \frac{2\bar{u}u'\tan\phi}{a} + F_\phi \\ C_3 &= \frac{-1}{\Gamma_0}\left(\frac{\bar{u}}{a\cos\phi}\frac{\partial T'}{\partial\lambda} + \frac{v'}{a}\frac{\partial\bar{T}}{\partial\phi}\right) + \frac{\omega'}{\Gamma_0}\left(\frac{\kappa\bar{T}}{1+\sigma} - \frac{\partial\bar{T}}{\partial\sigma}\right) \\ &\quad + \frac{Q}{\Gamma_0 C_p} + \frac{F_T}{\Gamma_0} \\ \Gamma_0 &= \frac{\kappa T_0}{1+\sigma} - \frac{dT_0}{d\sigma} \\ \nabla\cdot\mathbf{V}' &= \frac{1}{a\cos\phi}\left[\frac{\partial u'}{\partial\lambda} + \frac{\partial}{\partial\phi}(v'\cos\phi)\right] \end{aligned}\right\} \quad (2.7)$$

In (2.7), Γ_0 denotes a measure of the static stability of the standard atmosphere with $\kappa = R/C_p$, where R and C_p stand for the specific gas constant and the specific heat at constant pressure. The zonal and meridional components of frictional force are given by F_λ and F_ϕ. The rate of heating is denoted by Q. The thermal dissipation is treated separately and is denoted by F_T. The perturbation temperature T' is expressed by

$$T' = -\frac{g(1+\sigma)}{R}\frac{\partial z'}{\partial\sigma}. \quad (2.8)$$

Next, we introduce dimensionless variables to perturbation quantities

$$\left.\begin{aligned} &\tilde{u} = u'/(gH_*)^{1/2}, \quad \text{similarly for } \tilde{v} \\ &\tilde{z} = z'/H_* \\ &\tilde{\omega} = a\omega'/(gH_*)^{1/2} \\ &\tilde{T} = T'/T_* \\ &\tilde{t} = 2\Omega t \end{aligned}\right\}, \quad (2.9a)$$

where H_* is a scaling height chosen as 10 km and $T_* = gH_*/R$. We also introduce the following dimensionless variables

$$\left.\begin{aligned} &\bar{\alpha} = \bar{u}/(2a\Omega\cos\phi) \\ &\bar{H} = \bar{z}/H_* \\ &\bar{\tau} = \bar{T}/T_*, \quad \tau_0 = T_0/T_* \\ &S = \Gamma_0/T_* \end{aligned}\right\}. \quad (2.9b)$$

Dimensionless forms of the momentum and thermal dissipation terms and the heating term are expressed by

$$\left.\begin{aligned} &\tilde{F}_\lambda = F_\lambda/[2\Omega(gH_*)^{1/2}], \quad \text{similarly for } \tilde{F}_\phi \\ &\tilde{F}_T = F_T/(2\Omega T_*) \\ &\tilde{Q} = Q/(2\Omega C_p T_*) \end{aligned}\right\}. \quad (2.9c)$$

The system of equations (2.6) is then expressed in the following dimensionless form

$$\left.\begin{aligned} &\frac{\partial\tilde{u}}{\partial\tilde{t}} - \sin\phi\tilde{v} + \gamma\frac{\partial\tilde{z}}{\cos\phi\partial\lambda} = A + \tilde{F}_\lambda \\ &\frac{\partial\tilde{v}}{\partial\tilde{t}} + \sin\phi\tilde{u} + \gamma\frac{\partial\tilde{z}}{\partial\phi} = B + \tilde{F}_\phi \\ &\frac{\partial}{\partial\tilde{t}}\left[-\frac{\partial}{\partial\sigma}\left(\frac{1+\sigma}{S}\frac{\partial\tilde{z}}{\partial\sigma}\right)\right] + \gamma\tilde{\nabla}\cdot\tilde{\mathbf{V}} = \frac{\partial C}{\partial\sigma} + \frac{\partial}{\partial\sigma}\left(\frac{\tilde{F}_T}{S}\right) \end{aligned}\right\}, \quad (2.10)$$

where

$$\left.\begin{aligned} A &= -\bar{\alpha}\frac{\partial\tilde{u}}{\partial\lambda} + \left(2\bar{\alpha}\sin\phi - \cos\phi\frac{\partial\bar{\alpha}}{\partial\phi}\right)\tilde{v} \\ B &= -\bar{\alpha}\frac{\partial\tilde{v}}{\partial\lambda} - 2\bar{\alpha}\sin\phi\tilde{u} \\ C &= \frac{-1}{S}\left(\bar{\alpha}\frac{\partial\tilde{T}}{\partial\lambda} + \gamma\tilde{v}\frac{\partial\bar{\tau}}{\partial\phi}\right) + \frac{\tilde{Q}}{S} \\ \tilde{T} &= -(1+\sigma)\partial\tilde{z}/\partial\sigma \\ \gamma &= (gH_*)^{1/2}/(2a\Omega) \\ \tilde{\nabla}\cdot &= a\nabla\cdot \end{aligned}\right\}. \quad (2.11)$$

In A and C of (2.11), we neglected from C_1 and C_3 in (2.7) two vertical transport terms involving ω', which are small by scaling considerations.

3. Forced solutions

Our objective is to obtain the steady state response of the system (2.10)–(2.11) for a prescribed heating distribution Q. In K84 we investigated the same problem, except the basic state was treated as an atmosphere at rest. In that case, the terms A, B and C were all zero except the heating term Q. In the present case, we will take into account the effect of basic zonal flow. The case of no basic zonal flow was solved by using the method of three-dimensional normal mode expansion. This solution technique highlights the coupling effect of vertical normal modes through the vertical shear of basic zonal flow.

We assume that the heating takes the form

$$Q = C_p f(p) H(\phi) A_s e^{is\lambda}, \quad (3.1)$$

where A_s represents the Fourier coefficient for wavenumber s expressed in units of K s^{-1}. The vertical dependence factor $f(p)$ in the form of a parabola and the meridional dependence factor $H(\phi)$ with an exponential decay are the same as (3.2) and (3.4) in K84.

In order to solve the system of equations (2.10), we assume that $\tilde{u}$, $\tilde{v}$ and $\tilde{z}$ are expressed by

$$\left.\begin{aligned}\tilde{u}&=\sum_{n=1}^{N}\frac{1}{\sqrt{\lambda_n}}\hat{u}_n(\lambda,\phi,t)\Phi_n(\sigma)\\ \tilde{v}&=\sum_{n=1}^{N}\frac{1}{\sqrt{\lambda_n}}\hat{v}_n(\lambda,\phi,t)\Phi_n(\sigma)\\ \tilde{z}&=\sum_{n=1}^{N}\frac{1}{\lambda_n}\tilde{z}_n(\lambda,\phi,t)\Phi_n(\sigma)\end{aligned}\right\},\tag{3.2}$$

where $\Phi_n(\sigma)$ satisfies the vertical structure equation

$$\frac{d}{d\sigma}\left(\frac{1+\sigma}{S}\frac{d\Phi_n}{d\sigma}\right)+\lambda_n\Phi_n=0,\quad n=1,\cdots,N\tag{3.3}$$

where $\lambda_n = H_*/D_n$ and parameter D_n represents the equivalent height. Integer N denotes the number of vertical modes. The characteristics and solutions of (3.3) are discussed in detail in K84.

By substituting (3.2) into (2.10), multiplying by $\Phi_k(\sigma)$, integrating the results with respect to σ, and utilizing the orthogonality of $\Phi_n(\sigma)$, we obtain the system of horizontal equations governing each vertical mode:

$$\left.\begin{aligned}&\frac{\partial\hat{u}_n}{\partial\tilde{t}}-\sin\phi\hat{v}_n+\gamma_n\frac{\partial\hat{z}_n}{\cos\phi\partial\lambda}=F_u-k_c\hat{u}_n\\ &\frac{\partial\hat{v}_n}{\partial\tilde{t}}+\sin\phi\hat{u}_n+\gamma_n\frac{\partial\hat{z}_n}{\partial\phi}=F_v-k_c\hat{v}_n\\ &\frac{\partial\hat{z}_n}{\partial\tilde{t}}+\gamma_n\tilde{\nabla}\cdot\hat{\mathbf{V}}_n=F_z-k_c\hat{z}_n\end{aligned}\right\},\tag{3.4}$$

where

$$\gamma_n=\gamma/\lambda_n^{1/2}=(gD_n)^{1/2}/(2a\Omega)\tag{3.5}$$

and k_c denotes a dimensionless form of the dissipation coefficient. Here, as in K84, the effects of momentum and thermal dissipation are expressed through the Rayleigh friction and Newtonian cooling parameterizations.

In (3.4), F_u, F_v and F_z are expressed by

$$\left.\begin{aligned}F_u&=\sqrt{\lambda_n}\int_{-1}^{1}A\Phi_n(\sigma)d\sigma\\ F_v&=\sqrt{\lambda_n}\int_{-1}^{1}B\Phi_n(\sigma)d\sigma\\ F_z&=\int_{-1}^{1}\frac{\partial C}{\partial\sigma}\Phi_n(\sigma)d\sigma\end{aligned}\right\}.\tag{3.6}$$

The forms of A, B and C are given in (2.11). A further manipulation of $\partial C/\partial\sigma$ by separating the heating term from the rest yields

$$F_z=\int_{-1}^{1}\left(\frac{\partial C}{\partial\sigma}\right)_{WTQ}\Phi_n(\sigma)d\sigma-\int_{-1}^{1}\frac{\tilde{Q}}{S}\frac{d\Phi_n}{d\sigma}d\sigma,\tag{3.7}$$

where

$$\left(\frac{\partial C}{\partial\sigma}\right)_{WTQ}=\bar{\alpha}\frac{\partial}{\partial\lambda}\left[\frac{\partial}{\partial\sigma}\left(\frac{1+\sigma}{S}\frac{\partial\tilde{z}}{\partial\sigma}\right)\right]-\tilde{v}\frac{\partial}{\partial\sigma}\left(\frac{\gamma}{S}\frac{\partial\bar{\tau}}{\partial\phi}\right).\tag{3.8}$$

In deriving the last term of (3.7), we assumed that $\tilde{Q} = 0$ at $\sigma = \pm1$. We assume that the zonal flow is expressed by

$$\begin{aligned}\bar{\alpha}(\phi,\sigma)&=\alpha_0(\phi)(1-\Lambda\sigma)\\ &=\alpha_0(\phi)\sum_{l=1}^{N}\beta_l\Phi_l(\sigma),\end{aligned}\tag{3.9}$$

where $\bar{\alpha}_0(\phi)$ denotes the dimensionless basic-flow angular velocity at the level $\sigma = 0$, which is equivalent to the 500 mb level. The vertical shear is assumed to be constant, with Λ denoting the dimensionless shear parameter. The linear wind profile is then expanded by the vertical structure functions. The coefficients of the expansion are given by

$$\beta_l=\int_{-1}^{1}(1-\Lambda\sigma)\Phi_l(\sigma)d\sigma.\tag{3.10}$$

We seek the steady state solutions of (3.4) in response to a prescribed heating Q. By introducing the vectors

$$\begin{aligned}\mathbf{F}_n&=(F_u,F_v,F_z)^{\mathrm{T}},\\ \mathbf{W}_n&=(\hat{u}_n,\hat{v}_n,\hat{z}_n)^{\mathrm{T}},\end{aligned}\tag{3.11}$$

the steady state system of (3.4) can be represented by

$$\mathbf{L}_n\mathbf{W}_n=\mathbf{F}_n-k_c\mathbf{W}_n,\tag{3.12}$$

where $\mathbf{L}_n$ is the linear differential matrix operator as defined by (2.22) in K84.

The solutions $\mathbf{W}_n$ of (3.12) will be sought by expanding $\mathbf{W}_n$ in terms of Hough vector functions

$$\mathbf{W}_n(\phi)=\sum_{r=1}^{R}W_r^s(n)\mathrm{H}_r^s(\phi;n),\tag{3.13}$$

where

$$\mathrm{H}_r^s(\phi;n)=[U_r^s(\phi;n),-iV_r^s(\phi;n),Z_r^s(\phi;n)]^{\mathrm{T}}\tag{3.14}$$

using the same notation as in K84. The summation for serial number r from 1 to R should contain all meridional modes of the westward- and eastward-propagating gravity waves and rotational waves. The advantage of adopting the Hough expansion is that the matrix operator $\mathbf{L}_n\mathrm{H}_r^s$ forms the eigenvalue–eigenfunction problem

$$[\mathbf{L}_n-i\nu_r^s(n)]\mathrm{H}_r^s(\phi;n)=0,\tag{3.15}$$

where ν_r^s denotes the dimensionless frequency (≡ frequency divided by 2Ω).

Substituting (3.13) into (3.12), integrating the resulting equation with respect to μ (≡ $\sin\phi$) between $\mu = \pm1$ after multiplying the complex conjugate H_r^{s*}, and utilizing the fact that H_r^s and ν_r^s satisfy (3.15) and the orthogonality of H_r^s, we obtain

$$[iv^s_r(n)+k_c]W^s_r(n)=\int_{-1}^{1}\mathbf{F}_n\cdot\mathbf{H}^{s*}_r(\phi;n)d\mu \quad (3.16)$$

for each vertical mode $n = 1, 2, \cdots, N$.

The right-hand side of (3.16) must be expressed explicitly in terms of the vertical expansion (3.2) and the horizontal expansion (3.13) by utilizing the relationships (3.6)–(3.9). The result is

$$[iv^s_{r'}(n)+k_c]W^s_{r'}(n)+\sum_{k=1}^{N}\sum_{r=1}^{R}i\mathbf{b}^s_{r'r}(n,k)W^s_r(k)$$

$$=-\tilde{A}_S Q_n\int_{-1}^{1}H(\phi)Z^s_{r'}(\phi;n)d\mu \quad (3.17)$$

for $r' = 1, 2, \cdots, R$; $n = 1, 2, \cdots, N$. The form of matrix $\mathbf{b}^s_{r'r}(n,k)$ and the forcing function Q_n are given in the Appendix.

Once $\mathbf{W}_r^s$ is determined from (3.17), the three-dimensional solutions are represented by

$$[u'(\lambda,\phi,\sigma),v'(\lambda,\phi,\sigma),z'(\lambda,\phi,\sigma)]^{\mathrm{T}}$$

$$=\sum_{n=1}^{N}\mathbf{S}_n\sum_{r=1}^{R}W^s_r(n)\mathrm{H}^s_r(\phi;n)\Phi_n(\sigma)e^{is\lambda}, \quad (3.18)$$

where $\mathbf{S}_n$ denotes the scaling matrix

$$\mathbf{S}_n=\begin{bmatrix}(gD_n)^{1/2} & 0 & 0\\ 0 & (gD_n)^{1/2} & 0\\ 0 & 0 & D_n\end{bmatrix}. \quad (3.19)$$

As in K84, the globally averaged total energy $\overline{TE}$ is expressed by

$$\overline{TE}=\sum_{n=1}^{N}\sum_{r=1}^{R}(TE^s_r)_n, \quad (3.20)$$

where

$$(TE^s_r)_n=\frac{1}{2}gD_nW^s_rW^{s*}_r. \quad (3.21)$$

4. Numerical results

In the numerical results which follow, we consider a heating pattern with zonal wavenumber 2. We adopt the same symmetric heating distribution with respect to the equator as discussed in K84. Figure 1 shows the horizontal distribution of Q/C_p without the vertical dependence term $f(p)$ in (3.1). The contour interval is 0.4×10^{-5} K s^{-1} (=0.346 K d^{-1}). The vertical dependence term $f(p)$ is parabolic with respect to the pressure with $f(p)$ being zero at 1000 and 200 mb. The maximum value of $f(p)$ occurs at $p = 600$ mb and is 30/16, and this factor should be multiplied to obtain the heating or cooling at its maximum level.

We use the first six vertical modes as described in K84. For the meridional resolution, we selected a total of 17 modes, consisting of 16 rotational modes plus the Kelvin mode for each vertical mode. It was shown in K84 that the gravity modes, except the Kelvin mode, do not play important roles for slow heating. In the present case, we consider only the stationary response to heating. Therefore, we can neglect the contribution of gravity modes except for the Kelvin mode. The number of rotational modes is decided based on the spectral distribution of atmospheric energy (Tanaka, 1985) in terms of rotational modes. The rotational modes include both the symmetric and antisymmetric components with respect to the equator. Although the heating pattern used in this calculation is symmetric with respect to the equator, responses to a symmetric heating are not going to be symmetric, since the basic zonal flow in the calculation is not necessarily symmetric.

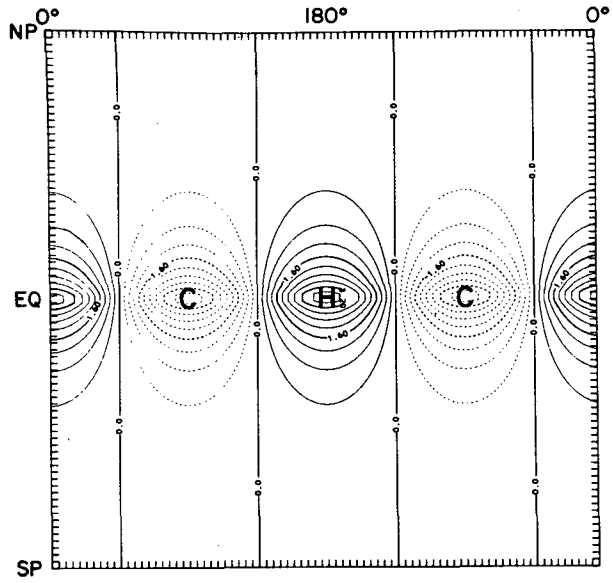

FIG. 1. Horizontal distribution of Q/C_p without the vertical dependence term $f(p)$ in (3.1).

a. Case of no basic zonal flow

In this case, we will reproduce essentially the same result given in K84 by considering the total of 17 meridional components per vertical mode instead of 36 meridional components per vertical mode used in K84. Figure 2a shows the flow pattern at the 870 mb level by superimposing the velocity field in arrows over the isobaric height in meters. The wind field indicates a low-level convergence (divergence) over the area of heating (cooling). We notice a strong zonal flow in the equatorial region. Away from the equator, the flow is quasi-geostrophic in relation to the height field. Although low pressure prevails over the heating areas, the maximum low pressure does not appear over the equator, but is shifted outside the tropics.

Figure 2b shows the flow pattern at the 227 mb level. The flow at this level is generally opposite to that at the lower level. This reflects the fact that the forced

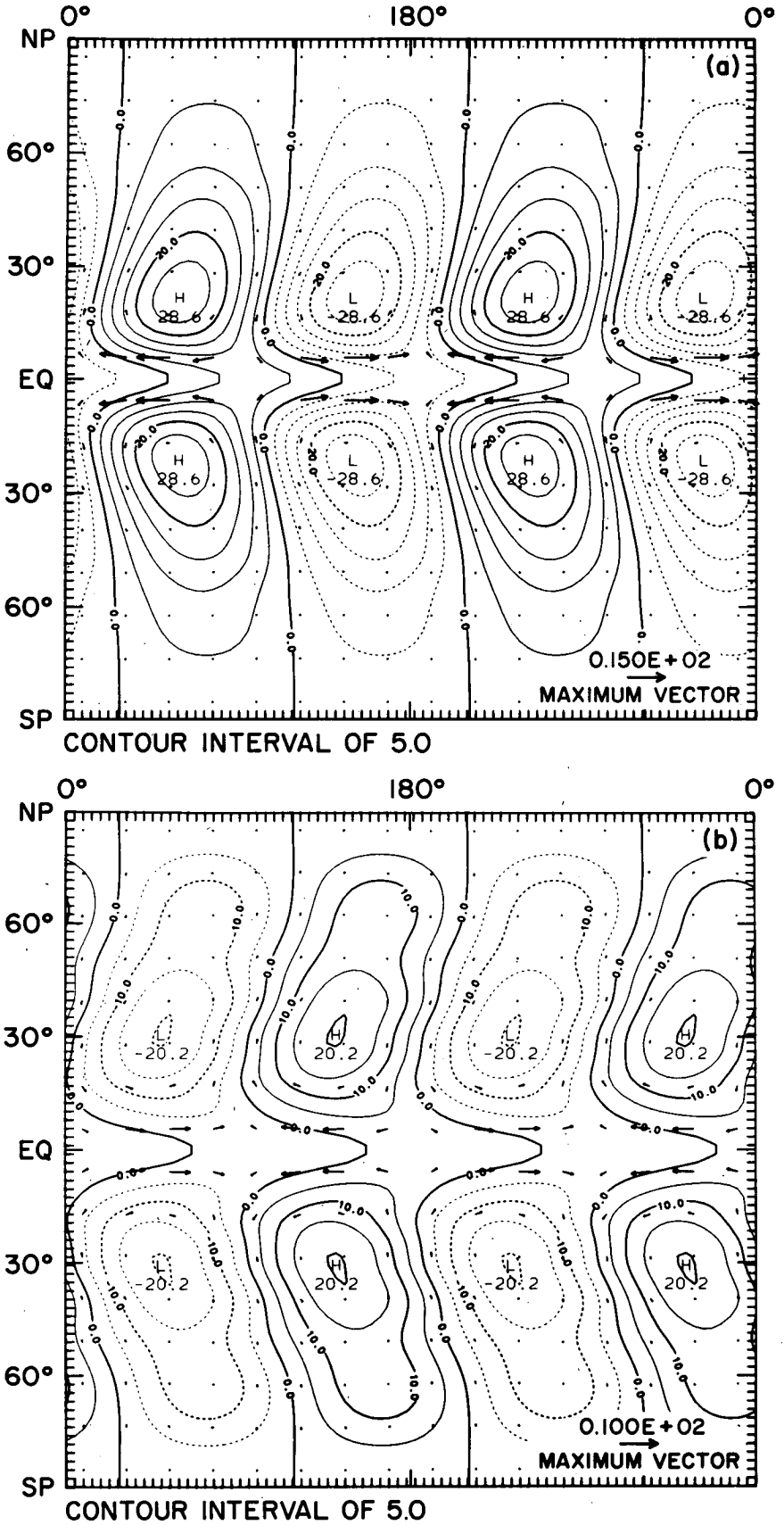

FIG. 2. (a) Flow pattern at the 870 mb level for the case of no basic zonal flow. Solid (dashed) lines show positive (negative) isobaric height contours with intervals of 5 m. Arrows represent wind vectors with the velocity scale of 15 m s^{-1} shown at the lower right-hand corner. (b) Flow pattern at the 227 mb level for the same case. The velocity scale is 10 m s^{-1}.

motion is dominated by the internal mode whose vertical profile is typically "baroclinic." Both Figs. 2a, b agree well with Figs. 3a, b, respectively, of K84. This reflects the fact that the contributions of gravity waves except the Kelvin wave in each vertical mode are negligible in a slow forcing problem. In fact, the present model carries 16 rotational components instead of 12 in K84. Therefore, Figs. 2a, b are more accurate than Figs. 3a, b of K84, despite the fact that the number of the total meridional components used in the present calculation is smaller than that used in K84.

b. *Case of* DJF *basic zonal flow with vertical shear* $\Lambda = 1$ *in (3.9)*

We show now the results of calculations including the zonal flow with vertical shear parameter $\Lambda = 1$ in (3.9). This means that the zonal flow is linear with respect to a vertical coordinate σ with $\bar{\alpha}(\phi) = 0$ at the surface level, $p = p_s$. As the meridional profile of the zonal flow $\bar{\alpha}_0(\phi)$, we choose the climatological zonal wind distribution at 500 mb for December, January and February (DJF) shown in Fig. 3, which was used in Kasahara (1980).

Figures 4a, b show the flow patterns for this case at the 870 and 227 mb levels, respectively. Comparisons of Fig. 4a with Fig. 2a and Fig. 4b with Fig. 2b reveal a number of features unique to the case of the DJF zonal flow with vertical shear $\Lambda = 1$. Tropical responses of the equatorial heating are generally similar in both cases, but the tropical response in the present case is much more confined to the low latitude region than those in the case of no zonal flow. Again, the tropical response to the heating is "baroclinic," i.e., the upper-level flow is generally opposite to the low-level flow.

The most distinctive aspect of Figs. 4a, b is that the equatorial heating also produces a significant response in the middle to higher latitudes with the inclusion of zonal flow. Moreover, the midlatitude response of the equatorial heating is "barotropic," unlike the case of the tropical response. Notice that the midlatitude response is stronger in the Northern Hemisphere than in the Southern Hemisphere. We will discuss this aspect further in section 5.

General features of the isobaric height response to the equatorial heating seen in Figs. 4a, b agree with these found in Fig. 12 of Webster (1982), apart from obvious differences in the two calculations due mainly to the different heating distributions; one is a local forcing and the other a wavenumber 2 forcing.

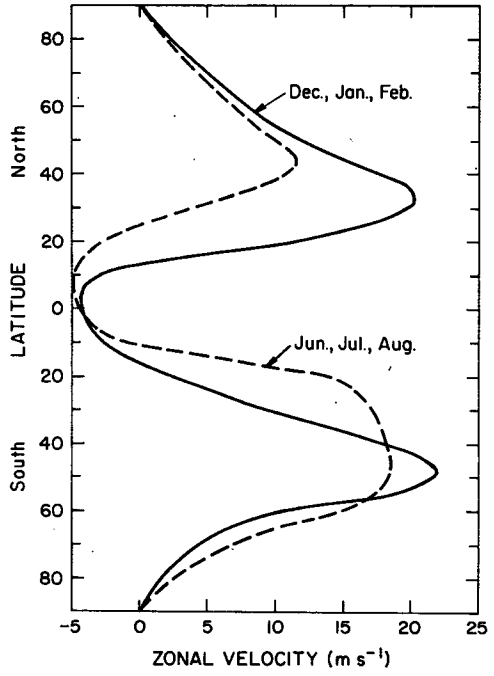

FIG. 3. Climatological zonal wind distribution at 500 mb. The solid line shows the distribution for December, January, February (DJF) and the dashed line for June, July, August (JJA). The source of data is given in Kasahara (1980).

c. *Case of* DJF *basic zonal flow with no vertical shear* $\Lambda = 0$ *in (3.9)*

In order to understand the impact of the basic zonal flow, we will show the results of calculations using the DJF basic flow without vertical shear $\Lambda = 0$ in (3.9). Figures 5a, b show the flow patterns at the 870 and 227 mb levels, respectively, in this case. Comparison between Figs. 4 and 5 indicates that a major difference is the absence of the middle to higher latitude response in the present case. Also, the low-level tropical response in the case of no vertical shear is much weaker than that in the DJF flow with vertical shear, while the upper-level tropical response is almost the same in its intensity in both cases.

d. *Energy considerations*

Because rather drastic changes occurred in the case of no vertical shear compared with the case of $\Lambda = 1$, it is instructive to show the spectral distribution of total energy $(TE_r^s)_n$ defined by (3.21) for both cases. Figure 6a shows this spectral distribution against the meridional index r for each vertical mode $n = 1$ to 6 for the case of $\Lambda = 1$. The meridional index $r = -1$ refers to the Kelvin mode, and $r = 0$ to 15 the rotational modes. The distribution for the external mode ($n = 1$) is shown by a solid line connecting the dots and that for the third internal mode ($n = 4$) by a dashed line connecting the triangles. Because the departure of the DJF zonal flow distribution from latitudinal symmetry with respect to the equator is small, the amounts of energy in antisymmetric modes $r = 0$, 2, 4, etc. are relatively small. The amounts of energy in the external mode, shown by the solid line, are much less than those in the lower vertical modes in a lower meridional index regime (say $r = -1$ to 3), but the amounts of external mode energy in the higher meridional index regime, say beyond $r = 4$, are comparable to or even higher than those of the internal vertical modes.

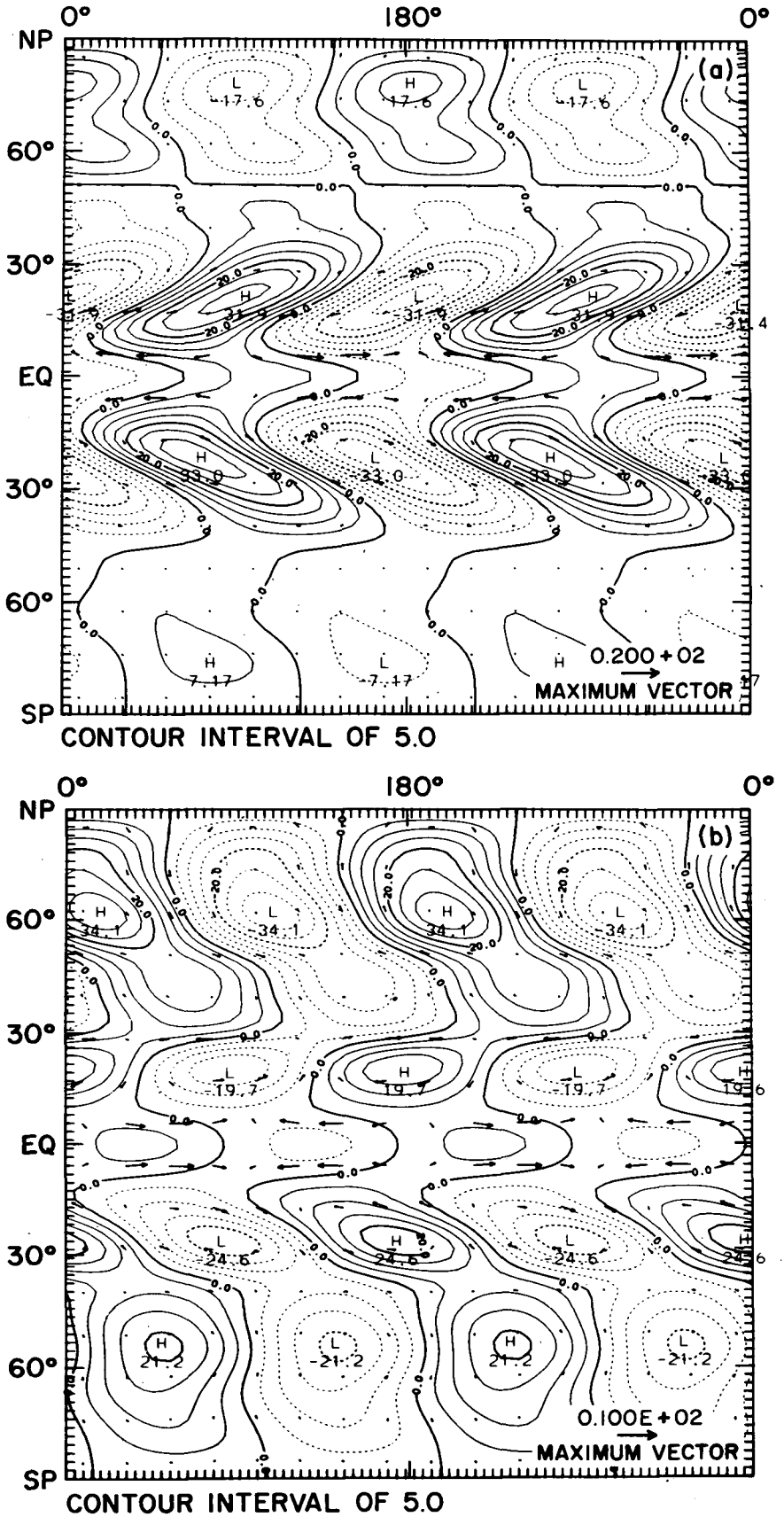

FIG. 4. (a) Flow pattern at the 870 mb level for the DJF zonal flow with vertical shear $\Lambda = 1$. The velocity scale is 20 m s^{-1}. Compare with Fig. 2a. (b) Flow pattern at the 227 mb level for the same case. The velocity scale is 10 m s^{-1}. Compare with Fig. 2b.

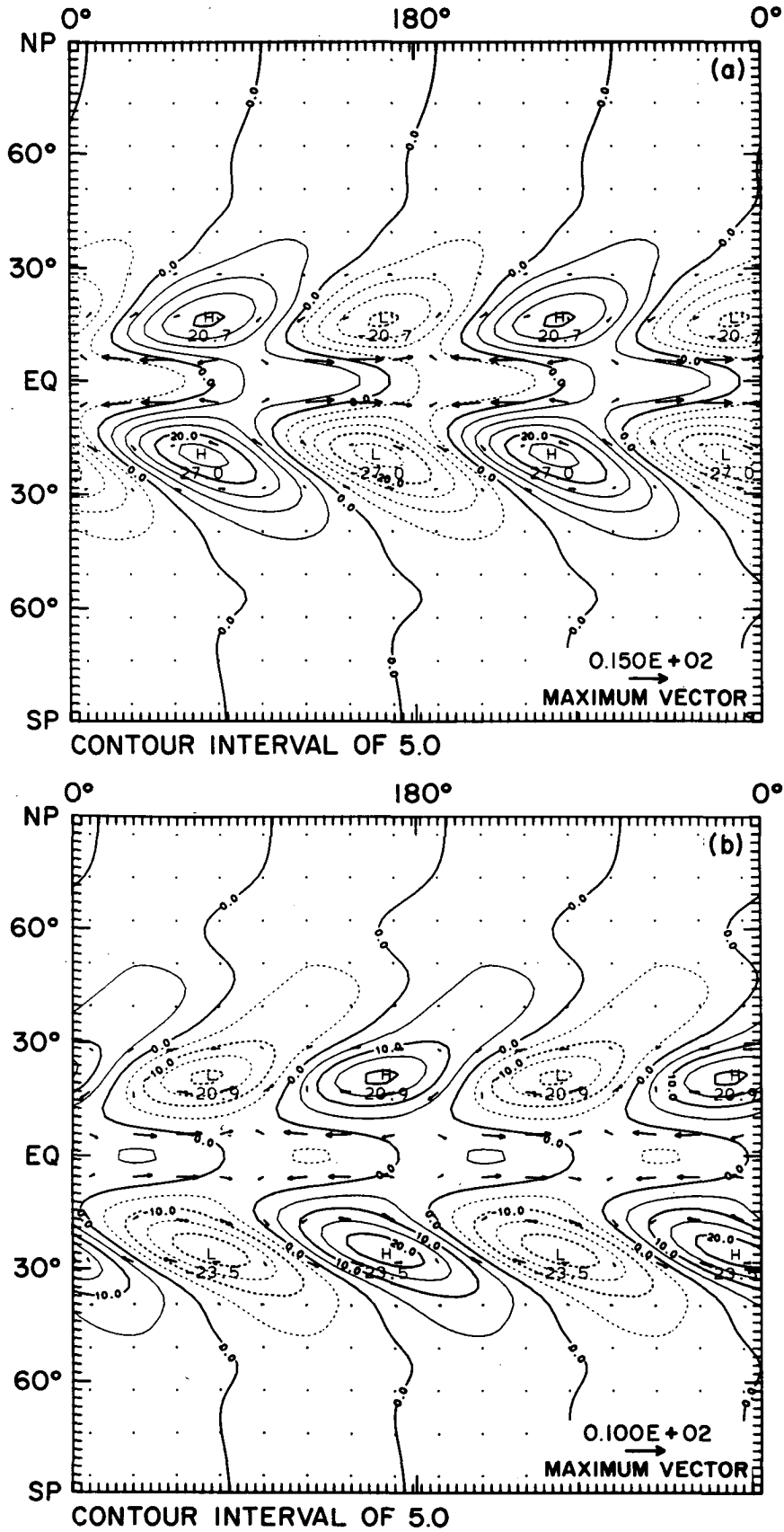

FIG. 5. As in Fig. 4 but with no vertical shear $\Lambda = 0$. (a) The velocity scale is 15 m s^{-1}. (b) The velocity scale is 10 m s^{-1}.

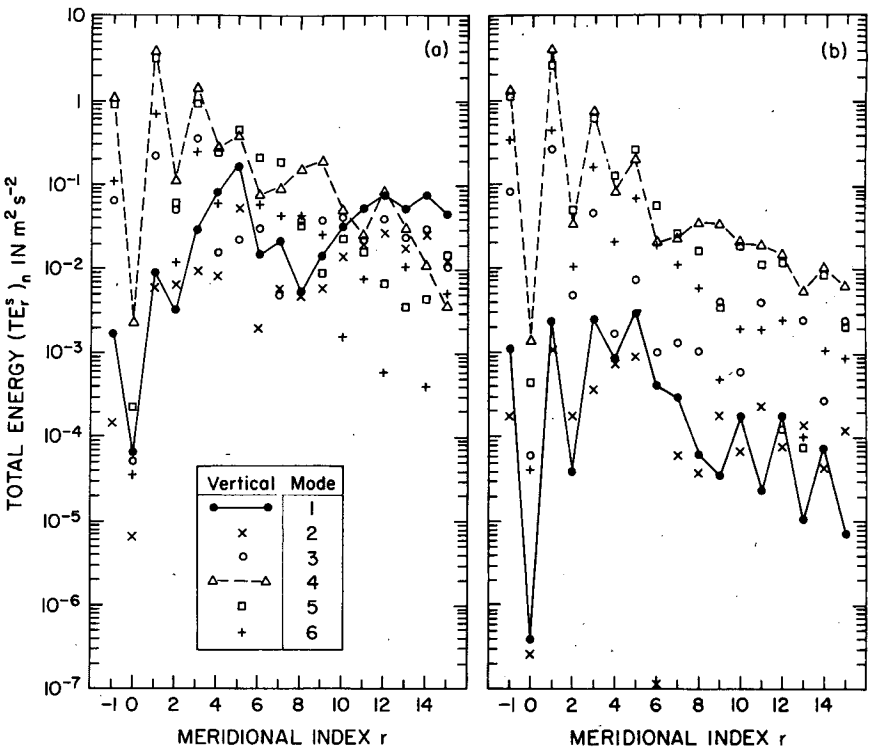

FIG. 6. The spectral distribution of total energy $(TE_r^2)_n$ defined by (3.24) in the case of DJF basic flow (a) with vertical shear $\Lambda = 1$ and (b) without vertical shear $\Lambda = 0$. The abscissa denotes the meridional index. The index $r = -1$ represents the Kelvin wave, and $r = 0$ to 15 the rotational waves. Symbols to denote vertical modes $n = 1$ to 6 are shown in the inset.

Figure 6b shows the same as Fig. 6a, except for the case of DJF basic flow without vertical shear. The most noticeable changes in Fig. 6b are that the amounts of the external mode energy are considerably decreased, while those of higher vertical modes are more or less unchanged.

Figure 7 shows the total energy summed with respect to meridional index from $r = -1$ to 15 as a function of vertical mode n in the abscissa. The heavy dashed line shows the case of DJF basic flow with vertical shear $\Lambda = 1$ and the thin dashed line the same DJF flow but without vertical shear. In addition, the case of no zonal flow is presented by a solid line. It is clear that the amounts of total energy for the vertical modes $n = 1$ to 3 increased substantially due to the vertical shear, while those for the vertical modes $n = 4$ to 6 are hardly affected. It is of interest to find, as far as the total energy distribution is concerned, that the case of no zonal flow is similar to the case of DJF basic flow without vertical shear.

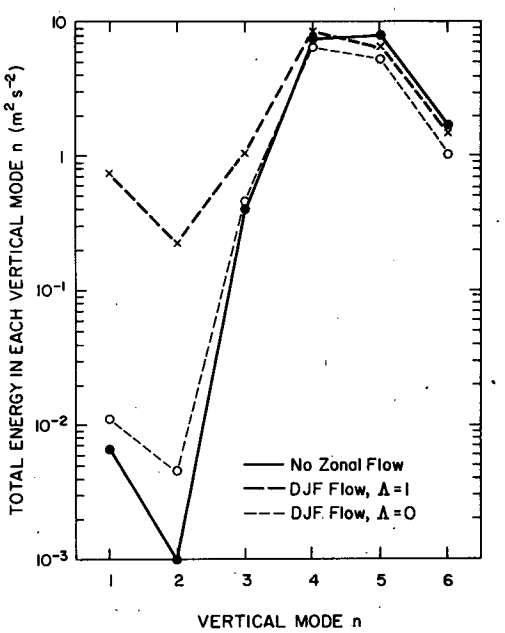

FIG. 7. The total energy summed with respect to the meridional index from $r = -1$ to 15 as a function of vertical mode n in the abscissa. The three cases of no zonal flow, DJF flow with vertical shear ($\Lambda = 1$), and DJF flow without shear ($\Lambda = 0$) are shown by the solid, heavy dashed, and thin dashed lines, respectively.

e. Effects of the zonal flow vertical shear

Both Figs. 6 and 7 indicate clearly a profound effect of the vertical shear of zonal flow. The key factors revealing the effects of the vertical shear of zonal flow

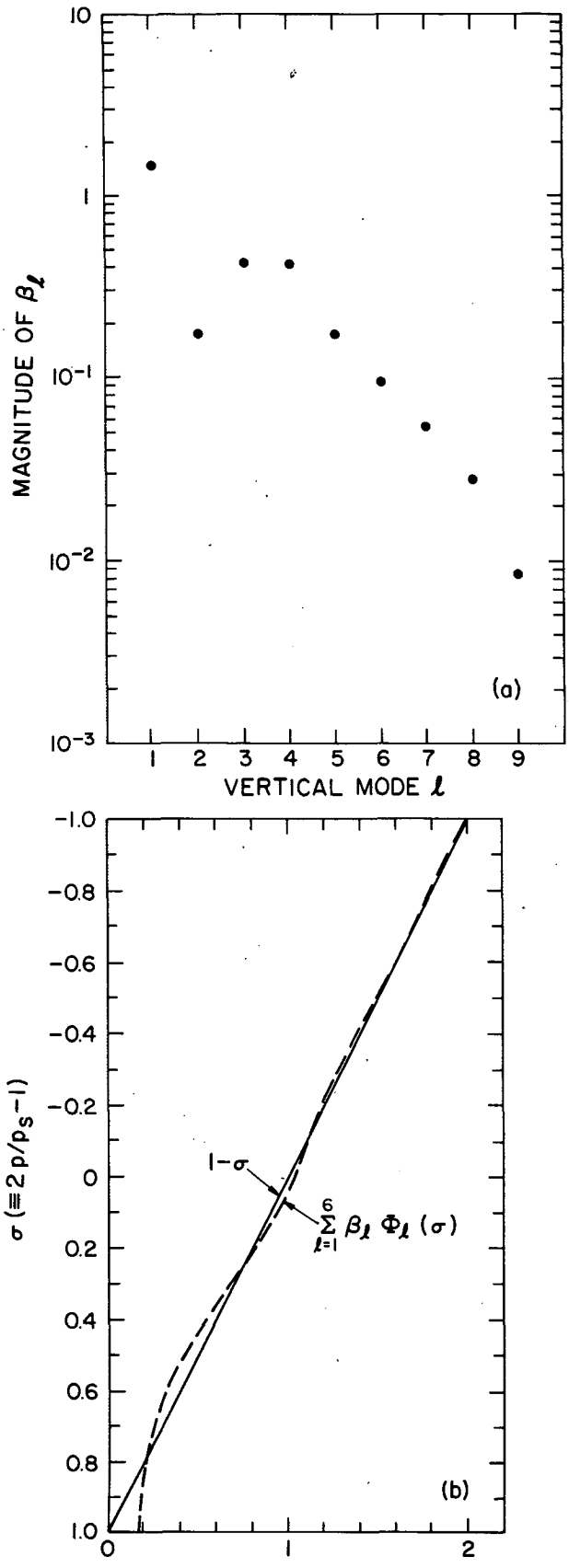

are 1) the expansion coefficients β_l defined by (3.10) and 2) the triple-interaction coefficients L_{lnk} defined by (A2).

Concerning the first factor, Fig. 8a shows the log distribution of β_l for the vertical linear profile $1 - \sigma$ as a function of vertical mode l. In the present calculation, we used only the first six vertical modes to expand the vertical profile $1 - \sigma$. The dashed line in Fig. 8b shows the composite of the vertical profile with six vertical modes $l = 1$ to 6. It approximates the linear profile reasonably well except for the lower atmosphere. It is seen from Fig. 8a that the external mode ($l = 1$) contribution is largest and the magnitude of β_l drops sharply as l increases. Hence, the neglect of the last three vertical modes may be justified for approximation of the linear wind profile.

Concerning the second factor for the $\Lambda = 1$ case, the values of the triple-interaction coefficients L_{lnk} for up to 6 in each vertical mode, l, n or k are shown in Table 1. The largest contribution in each l for the external mode ($n = 1$ row) is denoted by an asterisk. In all cases this maximum contribution occurs at $l = k$, and the order of magnitude is unity. For $n = 1$, the rest of the contributions are negligibly small. This means that the vertical shear interactions have all the same signs and only the self interactions contributed to $n = 1$. The situation is different for a higher vertical mode. For example, we denote the largest contribution in each l for the vertical mode $n = 4$ by a dagger. The largest contributions for $n = 4$ appear at $l = 1$ and $k = 4$ (similarly, $l = 4$ and $k = 1$), at $l = 2$ and $k = 3$ (similarly, $l = 3$ and $k = 2$) and at $l = 5$ and $k = 6$ (similarly, $l = 6$ and $k = 5$). This means that cross interactions are involved in addition to self interactions. In fact, the rest of the contributions for $n = 4$ are not so small. Hence, the contributions to $n = 4$ come from various interactions and the sum of all contributions may tend to be small due to cancellation. These findings may explain why the vertical shear so strongly affects the first few vertical modes, but not the higher vertical modes seen in Fig. 7.

It is clear that the effects of the zonal-flow vertical shear intensify the energy in the lower vertical modes (notably the external mode) through coupling between the lower and higher vertical modes. Earlier, Holton (1971) noted that the structure of the atmospheric perturbation in response to a given heating pattern is very sensitive to vertical shear of the zonal mean wind. The present finding also agrees with that of Lim and Chang (1986) in which the vertical shear of the zonal flow provides a mechanism of energy transfer from the internal mode motions to the external mode motions.

FIG. 8. (a) The log distribution of the magnitude of β_l for the linear vertical profile $1 - \sigma$ as a function of vertical mode l. (b) The solid line shows the linear vertical profile $1 - \sigma$, which can be reproduced by the expansion with nine vertical modes. The dashed line shows the representation of the profile with the first six vertical modes.

TABLE 1. The values of the triple-interaction coefficients L_{lnk} defined by (A2).

	k					
n	1	2	3	4	5	6
			l = 1			
1	0.75*	−0.18	0.01	−0.02	0.00	0.00
2	−0.18	1.08	0.14	0.03	0.03	−0.02
3	0.01	0.14	0.87	0.10	0.05	−0.04
4	−0.02	0.03	0.10	0.73†	0.06	−0.03
5	0.00	0.03	0.05	0.06	0.70	−0.05
6	0.00	−0.02	−0.04	−0.03	−0.05	0.68
			l = 2			
1	−0.18	1.08*	0.14	0.03	0.03	−0.02
2	1.08	−2.21	−0.90	−0.32	−0.20	0.17
3	0.14	−0.90	−0.75	−0.57	−0.36	0.28
4	0.03	−0.32	−0.57†	−0.03	−0.27	0.21
5	0.03	−0.20	−0.36	−0.27	0.14	0.18
6	−0.02	0.17	0.28	0.21	0.18	0.20
			l = 3			
1	0.01	0.14	0.87*	0.10	0.05	−0.04
2	0.14	−0.90	−0.75	−0.57	−0.36	0.28
3	0.87	−0.75	0.55	0.10	−0.25	0.23
4	0.10	−0.57†	0.11	0.07	0.23	−0.03
5	0.05	−0.36	−0.25	0.23	−0.02	−0.20
6	−0.04	0.28	0.23	−0.03	−0.20	−0.21
			l = 4			
1	−0.02	0.03	0.10	0.73*	0.06	−0.03
2	0.03	−0.32	−0.57	−0.03	−0.27	0.21
3	0.10	−0.57	0.10	0.07	0.23	−0.03
4	0.73†	−0.03	0.07	−0.43	−0.29	−0.23
5	0.06	−0.27	0.23	−0.29	−0.20	0.32
6	−0.03	0.21	−0.03	−0.23	0.32	0.00
			l = 5			
1	0.00	0.03	0.05	0.06	0.70*	−0.05
2	0.03	−0.20	−0.36	−0.27	0.14	0.18
3	0.05	−0.36	−0.25	0.23	−0.02	−0.20
4	0.06	−0.27	0.23	−0.29	−0.20	0.32†
5	0.70	0.14	−0.02	−0.20	0.17	−0.09
6	−0.05	0.18	−0.20	0.32	−0.09	0.11
			l = 6			
1	0.00	−0.02	−0.04	−0.03	−0.05	0.68*
2	−0.02	0.17	0.28	0.21	0.18	0.20
3	−0.04	0.28	0.23	−0.03	−0.20	−0.21
4	−0.03	0.21	−0.03	−0.23	0.32†	0.00
5	−0.05	0.18	−0.20	0.32	−0.09	0.11
6	0.68	0.20	−0.21	0.00	0.11	0.19

* Denotes the largest contribution in each l for the external node ($n = 1$ row).

† Denotes the largest contribution in each l for the vertical mode $n = 4$.

5. Horizontal propagation of stationary waves

In the previous section, we saw the response of planetary waves in the mid- to higher latitudes to stationary heating in the equatorial region in the case of DJF zonal flow with vertical shear $\Lambda = 1$. Moreover, the midlatitude response is stronger in the Northern Hemisphere than in the Southern Hemisphere. In the case of DJF zonal flow without vertical shear ($\Lambda = 0$), however, we find little midlatitude response. It is well known that the presence of a westerly zonal flow whose intensity is less than the critical value U_c is favorable to the meridional propagation of stationary planetary-scale waves, while the propagation is prohibited in an easterly regime (Charney, 1969). According to Dickinson (1980), the critical value is given by

$$U_c \approx 300 \text{ m s}^{-1}/(s^2+3), \tag{5.1}$$

where s is the zonal wavenumber. The values of U_c become 75, 43 and 25 m s^{-1} for $s = 1$, 2 and 3, respectively. Since we are concerned with $s = 2$ in this paper and the maximum westerly speed in the DJF profile is about 22 m s^{-1}, we can expect that planetary wave 2 generated by the tropical heating will be able to propagate into the midlatitudes. Although the use of the word "propagation" may not be appropriate for stationary wave solutions, one should look upon it as the process of reaching a stationary state when $t \to \infty$ in an initial value problem under a stationary forcing.

Because we found little midlatitude response for the DJF zonal flow without vertical shear ($\Lambda = 0$), a question may arise whether this result is in contradiction with the idea of meridional propagation of planetary-scale waves. We explore this question in this section.

Since the meridional structures of the higher internal modes are equatorially trapped, while those of the external mode (and also lower internal modes) are global, we first examine the horizontal flow patterns associated with the vertical mode n. Figure 9a shows the horizontal flow pattern of the external mode $n = 1$ in the case of DJF zonal flow with vertical shear $\Lambda = 1$. Solid (dashed) lines denote positive (negative) isobaric height contours with intervals of 5 m. Arrows represent wind vectors with the velocity scale of 2.5 m s^{-1} shown at the lower right-hand corner. Features of Fig. 9a are that the response to equatorial heating appears strongest in the higher latitudes and the tropical response is visible only in the wind field. Moreover, the wind response in the tropics does not appear to be as organized as in the higher latitudes.

Figure 9b shows the same as Fig. 9a, except for the third internal mode ($n = 4$). Note the velocity scale is 10 m s^{-1}. Recall that the vertical mode $n = 4$ is one of the most active components, together with $n = 5$, as seen in Fig. 7. The tropical responses in the height and wind fields are reminiscent of those shown by Gill (1980). The height field shows a weak midlatitude response, and the wind field associated with it is very weak. Figures 9a, b are instructive in understanding what is happening in Figs. 4a, b. It is clear that the "barotropic" response in the higher latitudes is generated mainly by the external mode $n = 1$ with some contributions from $n = 2$ and $n = 3$. On the other hand, the "baroclinic" response in the tropics is gen-

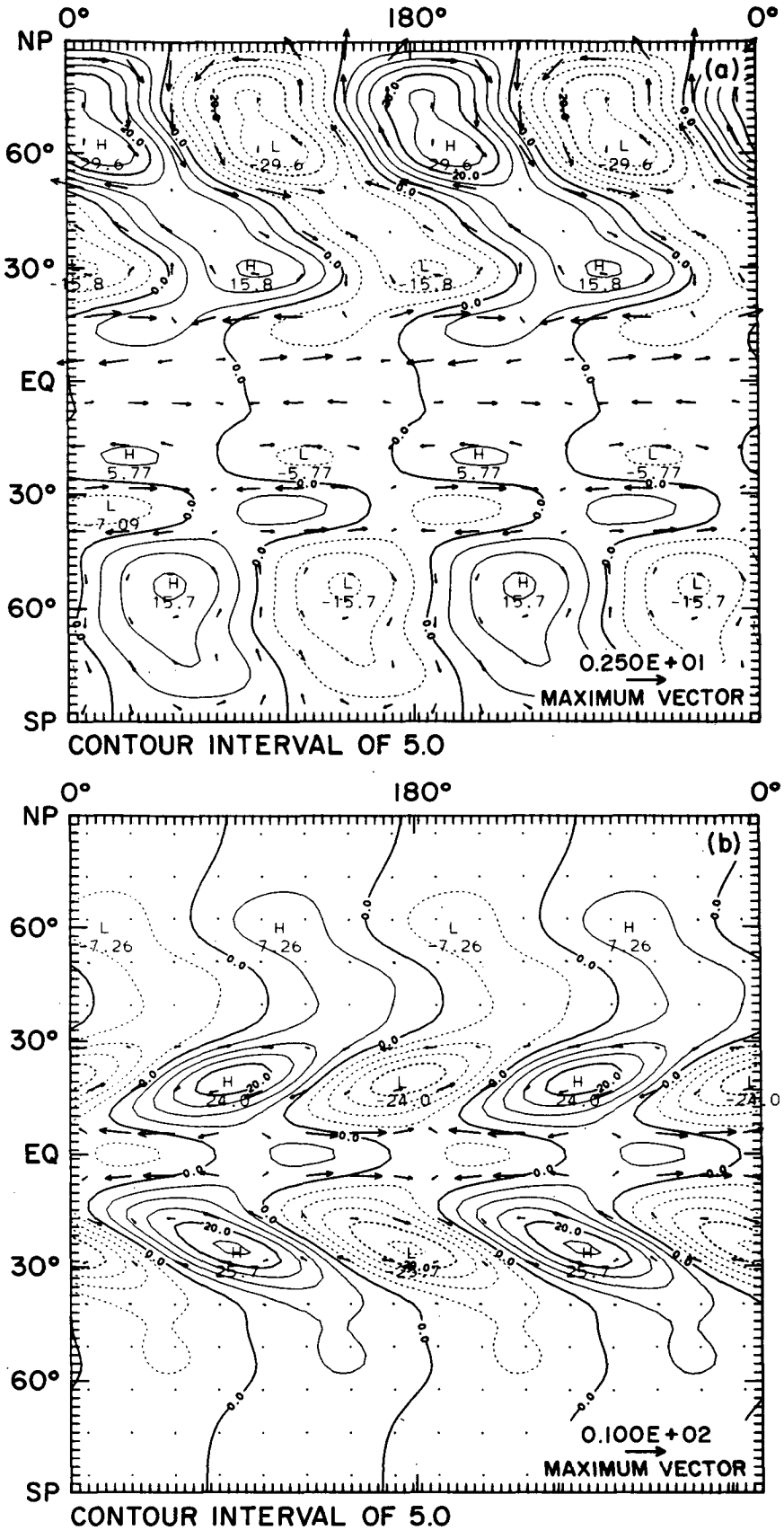

FIG. 9. (a) Flow pattern for the external mode $n = 1$ in the case of DJF zonal flow with vertical shear $\Lambda = 1$. Solid (dashed) lines denote positive (negative) height contours with intervals of 5 m. Arrows represent wind vectors with the velocity scale of 2.5 m s^{-1} shown at the lower right-hand corner. (b) As in (a) but for the third internal vertical mode ($n = 4$). The velocity scale is 10 m s^{-1}.

erated by the higher internal modes, mostly $n = 4$ and $n = 5$.

Let us then look at the same modal structures for the case of DJF zonal flow without vertical shear $\Lambda = 0$. Figure 10a shows the same as Fig. 9a, except for this case. Note that the contour interval is 0.5 m, a factor of 10 smaller than that in Fig. 9a, though the overall contour pattern is similar to that of Fig. 9a. It is clear that the meridional propagation of planetary waves generated by the tropical heating has indeed occurred in this case. However, due to the fact that the intensity of external mode $n = 1$ was weak, the response of the mid- to higher latitudes in the composite patterns shown in Figs. 5a, b is overshadowed by the strong local responses of higher internal modes. Figure 10b shows the same as Fig. 9b, except for the DJF case without vertical shear $\Lambda = 0$. Although the tropical response in this case is somewhat weaker than the DJF case with vertical shear $\Lambda = 1$, the response of this higher internal mode is less affected by the presence of zonal flow as implied also from Fig. 7.

We have seen that the meridional propagation of planetary waves occurs in the basic zonal flow, regardless of the wave intensity, as long as the basic zonal flow configuration is favorable. Moreover, the ability of planetary waves to propagate meridionally in the zonal flow depends also on the vertical mode. In order to examine the question of propagability somewhat more quantitatively, we will resort to the concept of refractive index.

By applying to the stationary system of equation (2.10) a quasi-geostrophic analysis similar to that by Matsuno (1970), we obtain

$$\bar{\alpha}\frac{\partial}{\partial\lambda}\left[\gamma\frac{\sin^2\phi}{\cos\phi}\frac{\partial}{\partial\phi}\left(\frac{\cos\phi}{\sin^2\phi}\frac{\partial\tilde{z}}{\partial\phi}\right)+\frac{\gamma}{\cos^2\phi}\frac{\partial^2\tilde{z}}{\partial\lambda^2}+\frac{\sin^2\phi}{\gamma}\frac{\partial}{\partial\sigma}\left(\frac{1+\sigma}{S}\frac{\partial\tilde{z}}{\partial\sigma}\right)\right]+\frac{\partial\bar{q}}{\partial\phi}\frac{\gamma}{\cos\phi}\frac{\partial\tilde{z}}{\partial\lambda}=0. \quad (5.2)$$

Here, we omitted the contributions of momentum dissipation and heating. Moreover, we will consider the basic zonal flow without vertical shear $\Lambda = 0$, so that the basic flow angular velocity $\bar{\alpha}$ will be replaced by $\bar{\alpha}_0(\phi)$. We have seen that the constant vertical shear of zonal flow did not affect very much the meridional propagation of energy. In the case of $\Lambda = 0$, the meridional gradient of the potential vorticity of basic flow $\partial\bar{q}/\partial\phi$ (in the dimensionless form adopted in this paper) becomes

$$\frac{d\bar{q}}{d\phi}=\cos\phi-\frac{d}{d\phi}\left(\cos\phi\frac{d\bar{\alpha}_0}{d\phi}-2\bar{\alpha}_0\sin\phi\right). \quad (5.3)$$

As adopted in (3.2), we express $\tilde{z}$ of (5.2) by the vertical modal expansion

$$\tilde{z}=\sum_n\frac{1}{\lambda_n}\hat{z}_n(\lambda,\phi)\Phi_n(\sigma) \quad (5.4)$$

and introduce the expression

$$\hat{z}_n(\lambda,\phi)=\sum_s h_n^s(\phi)e^{is\lambda}. \quad (5.5)$$

After substitutions of (5.4) and (5.5) into (5.2), utilization of the Fourier transform and the vertical structure equation (3.5), we obtain

$$\sum_n\left\{\bar{\alpha}_0\left[\frac{\sin^2\phi}{\cos\phi}\frac{d}{d\phi}\left(\frac{\cos\phi}{\sin^2\phi}\frac{dh_n^s}{d\phi}\right)-\frac{s^2}{\cos^2\phi}h_n^s-\frac{\sin^2\phi}{\gamma^2}\lambda_n h_n^s\right]\times\frac{1}{\lambda_n}\Phi_n+\frac{d\bar{q}}{d\phi}\frac{h_n^s}{\cos\phi}\frac{1}{\lambda_n}\Phi_n\right\}=0.$$

By multiplying the above equation by Φ_m, integrating the resultant equation with respect to σ from -1 to 1, and utilizing the orthogonality condition on Φ_n discussed in K84, we obtain

$$\frac{\sin^2\phi}{\cos\phi}\frac{d}{d\phi}\left(\frac{\cos\phi}{\sin^2\phi}\frac{dh_n^s}{d\phi}\right)+R_n^s h_n^s=0, \quad (5.6)$$

where

$$R_n^s=\frac{1}{\bar{\alpha}_0\cos\phi}\frac{d\bar{q}}{d\phi}-\frac{\sin^2\phi}{\gamma^2}\lambda_n-\frac{s^2}{\cos^2\phi} \quad (5.7)$$

denotes an index of refraction squared.

If $R_n^s < 0$, h_n^s will have an evanescent character. In order to observe a significant response in mid- to higher latitudes to tropical heating, the zonal flow configuration must be in such a condition that $R_n^s > 0$. The zonal wavenumber s appears only in the last term of (5.7), which is negative, so that longitudinally small-scale disturbances are not favorable to meridional propagation. Likewise, the inverse of the equivalent height λ_n ($\equiv H_*/D_n$) appears only in the second term on the right-hand side of (5.7) and this term is negative. Hence, disturbances with a small equivalent height are also not favorable to meridional propagation. The first term on the right-hand side of (5.7) represents a contribution of the zonal flow. Since $\cos\phi$ will usually dominate in the expression of $d\bar{q}/d\phi$ in (5.3) in lower latitudes, horizontal energy propagation will not be expected in the region of easterlies ($\bar{\alpha}_0 < 0$).

Figure 11a stipples the latitude ranges in which $R_n^s < 0$ for each vertical mode $n = 1$ to 6 in the case of DJF zonal flow. Since the heating distribution is symmetric and the stippled region in the tropics (in each n) is shifted southward, it is expected that meridional energy propagation is more active in the Northern Hemisphere than in the Southern Hemisphere. Since this analysis is applicable to the case of no vertical shear $\Lambda = 0$, let us interpret the modal structure of $n = 1$ shown in Fig. 10a in light of the R_n^s discriminant for $n = 1$ shown in Fig. 11a. We see on Fig. 10a that a strong height response appears in the Northern Hemisphere around 70°N, which is close to the northern edge of positive R_n^s in $n = 1$ on Fig. 11a. On the other hand, we see on Fig. 10a that the Southern Hemisphere

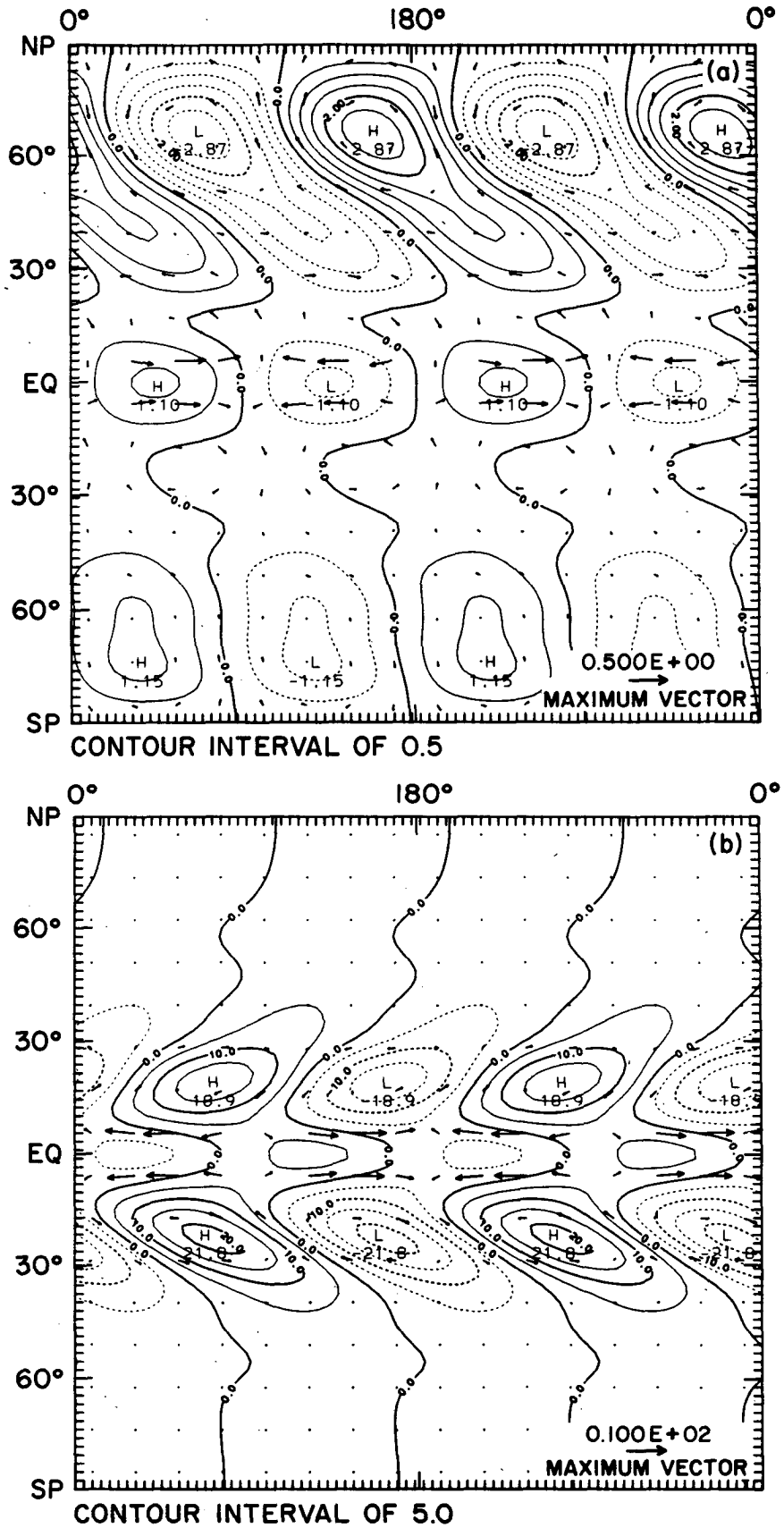

FIG. 10. As in Fig. 9 but in the case of DJF zonal flow without vertical shear $\Lambda = 0$. The height contour interval in (a) is 0.5 m and the velocity scale is 0.5 m s^{-1}.

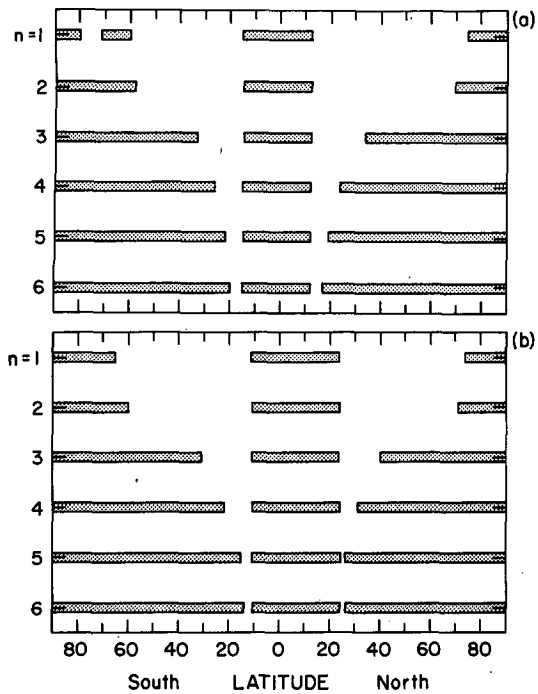

FIG. 11. (a) Latitude ranges where $R_n^s < 0$ are shown by stippling for different vertical modes $n = 1$ to 6. (a) In the case of DJF zonal flow without vertical shear $\Lambda = 0$. (b) In the case of JJA zonal wind profile with $\Lambda = 0$.

response, though it is weak, extends as far as 80°S. This situation may be expected by the fact that for $n = 1$ on Fig. 11a the southern edge of the positive R_n^s reaches 80°S, though the positive R_n^s region is interrupted by the negative R_n^s between 60° and 72°S. For vertical mode $n = 4$, the R_n^s discriminant shown in Fig. 11a appears useful in explaining the maximum response around 20° in both the Northern and Southern hemispheres.

Figure 11b shows the same as Fig. 11a, except for the case of June, July, August (JJA) zonal flow shown in Fig. 3. The negative R_n^s region in the tropics (in each n) is shifted northward. Hence, one expects a stronger response in the Southern Hemisphere to the symmetric heating used in the present study. However, the Northern Hemisphere midlatitude response would reach a latitude higher than the corresponding latitude to which the Southern Hemisphere midlatitude response would reach. This is expected from the R_n^s discriminant pattern for $n = 1$ and $n = 2$ shown in Fig. 11b.

Figures 12a, b show the flow patterns at the 870 and 227 mb levels, respectively, the same as Figs. 4a, b except for the JJA zonal flow with vertical shear $\Lambda = 1$. We see that the midlatitude response is greater in the Southern Hemisphere than the Northern Hemisphere, but the midlatitude response reaches higher in latitude in the Northern Hemisphere than the Southern Hemisphere. These observations are consistent with what would be expected from Fig. 11b.

6. Summary and discussion

The response of planetary waves to stationary tropospheric tropical heating was investigated using a stratified global atmospheric model linearized with respect to a basic mean zonal flow. The method of three-dimensional normal mode expansion was used to solve the basic equation in order to reveal modal characteristics of the solutions in the vertical direction as well as in the horizontal direction.

The basic mean zonal wind was represented by the product of meridional and vertical dependence terms in order to examine their roles separately. Climatological zonal wind distributions at the 500 mb level for December, January and February (DJF) and June, July and August (JJA) were used for the meridional dependence. The linear vertical profile with zero velocity at the 1000 mb level was adopted, except for the case of no vertical shear.

As the tropical heating distribution, we assumed a wavenumber 2 dependence in longitude and a symmetric bell shape in latitude with the maximum at the equator. The vertical distribution of heating was parabolic in pressure p with zero heating at $p = 200$ and 1000 mb.

Without the basic zonal flow, the internal vertical modes whose equivalent heights are on the order of a few hundred meters were favorably excited, but the response of the external mode ("barotropic" mode) was relatively small, in agreement with the conclusion of K84.

With inclusion of the basic zonal flow, the vertical shear of zonal flow permits the coupling of the external mode with the internal vertical modes. A significant response was obtained in the external mode through this coupling as a result of exciting the "baroclinic" internal modes by tropical heating. The present finding that the vertical shear of zonal flow provides a mechanism of energy transfer from the internal mode motions to the external mode motions is in agreement with Lim and Chang (1986).

The local response to tropical heating, such as an anticyclonic pair in the upper troposphere astride the equator, is explained by the excitation of the internal vertical modes. Their meridional structures are equatorially trapped, and the intensity of the response is less affected by the basic zonal flow. Hence, the findings of Gill (1980) are applicable to more general situations of the reference atmosphere with mean zonal flow.

Since the meridional structure of the external mode is global, a significant response of the external mode to tropical heating is not confined to the tropics. The direction of the basic zonal flow and its meridional shear has a profound influence on the meridional energy propagation of planetary waves as envisaged by Charney (1969). Our results show that the mid- to higher latitude response to tropical heating is mostly barotropic and that the remote response is stronger in

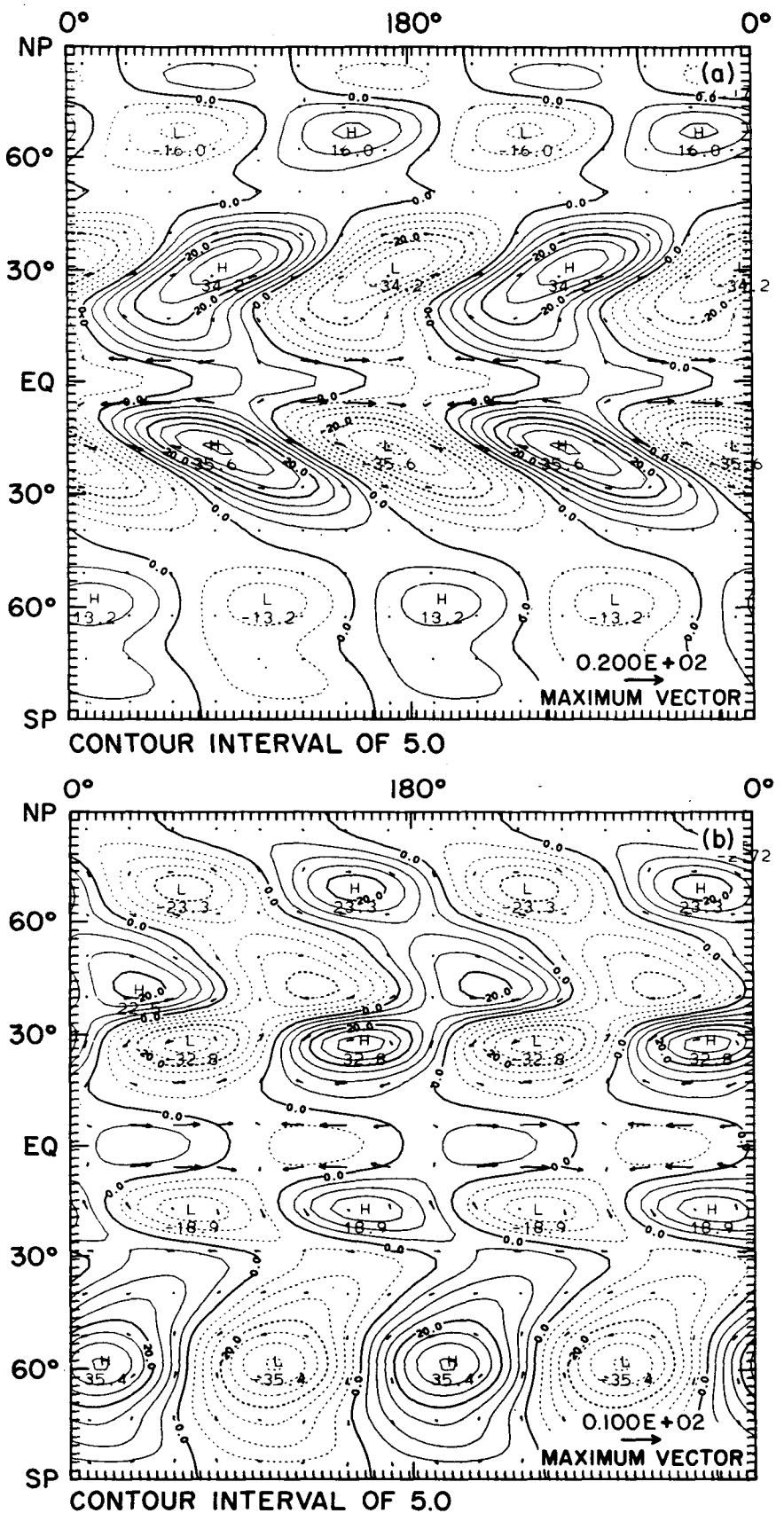

FIG. 12. (a) As in Fig. 2a but for the case of JJA zonal flow with vertical shear $\Lambda = 1$. The velocity scale is 20 m s^{-1}. (b) Flow pattern at the 227 mb level for the same case. The velocity scale is 10 m s^{-1}.

the Northern Hemisphere than in the Southern Hemisphere in the case of DJF zonal flow, and the reverse occurs in the case of JJA zonal flow. The propagability of zonal mean flow in order to produce a remote response was analyzed in section 5 using the concept of refractive index.

The present findings may serve to fill in a missing link in the dynamical theory of atmospheric teleconnections—correlations in atmospheric circulation anomalies over widely separated regions of the earth. Blackmon et al. (1983) investigated the response of a general circulation model (GCM) to warm sea surface temperature anomalies in the equatorial Pacific east of the dateline. Their results indicate that the mid- to higher latitude responses as well as the local response agree, in many respects, with the observed atmospheric anomaly pattern discussed in Horel and Wallace (1981).

Branstator (1985) examined the solutions of a linear, steady, global barotropic model under a prescribed tropical forcing. When a long-term mean zonally varying basic flow obtained from the GCM experiment of Blackmon et al. was used to linearize the barotropic vorticity equation, Branstator (1985) found that the midlatitude response of the GCM was well reproduced by the simple model. Since Branstator's (1985) model is barotropic and steady state, the midlatitude response to a prescribed tropical forcing can be interpreted by the mechanism of horizontal energy propagation in a barotropic atmosphere with meridional and zonal structure (Webster and Holton, 1982; Branstator, 1983). It is important to note here that, although no specific reference is made to the equivalent depth in the vorticity equation used by Branstator (1985), his formulation assumes that a prescribed tropical forcing is given to the Haurwitz mode (corresponding to the case of infinite equivalent height), which is essentially what is referred to as the external mode here.

When equatorial waters are unusually warm, such as during El Niño, cumulus convection tends to be anchored over the warm water, releasing latent heat of condensation that gives rise to thermal forcing. Planetary-scale waves will be generated by the anomalous heating and propagated into the midlatitudes. In order for this scenario to describe the process of atmospheric teleconnections, it is necessary to explain the excitation of the external mode by the anomalous heating as postulated by Branstator (1985). The present study suggests that the vertical shear of the basic zonal flow plays an important role in energy transfer to intensify the external mode as the result of exciting "baroclinic" internal modes by tropospheric tropical heating.

As an additional dynamical mechanism responsible for atmospheric teleconnections, Simmons et al. (1983) demonstrated that the teleconnection pattern appears as a preferable normal mode of barotropic instability in the zonally varying mean basic state. Therefore, the basic state provides energy for the disturbances. Although anomalous tropical forcing may not be the only way of exciting the preferred wave patterns, it can be looked upon as an effective source of excitation for the disturbances. Simmons et al. (1983) hypothesize that teleconnection patterns resembling unstable normal mode structures are favorable to excitation, because they are able to extract energy from the basic state. Therefore, one might expect to see evidence of these normal-modelike structures in long-term statistics.

It is not the intention of this paper to review the mechanism of atmospheric teleconnections. The question of barotropic and baroclinic instability in discussing the response of a time-dependent, baroclinic atmosphere to tropical thermal forcing is an important issue in the framework of a nonlinear model (Grose et al., 1984) that should be investigated separately. Nevertheless, it may be pertinent to comment here that application of the three-dimensional normal mode expansion to solving a time-dependent, baroclinic model of the atmosphere would be helpful in interpreting the modal characteristics in spectral space in the vertical direction as well as in the horizontal. A preliminary study based on a particular basic zonal wind distribution used by Simmons and Hoskins (1976) and Frederiksen (1978) shows that the three-dimensional normal mode formulation can be applicable to the problem of baroclinic–barotropic instability over the sphere.

Acknowledgments. Partial support for this research has been provided through the National Oceanic and Atmospheric Administration under N.O. NA85-AAG02575 and the U.S.–Brazil Cooperative Science Program, Division of International Programs, National Science Foundation. The authors wish to thank J. Tribbia, H. Tanaka, and G. Branstator for their useful discussions and comments regarding this research. The figures were drafted by the NCAR Graphics Department. The manuscript was typed by M. Niemczewski.

APPENDIX

Forms of Matrix $\mathbf{b}^{s}_{rr}(k, n)$ and Forcing Function Q_n

$$\mathbf{b}^{s}_{rr}(n,k) = \sum_l L_{lnk}\left(\frac{\lambda_n}{\lambda_k}\right)^{1/2}\beta_l\int_{-1}^{1}\Bigg[s\bar{\alpha}_0(\phi)\Big\{U^s_r(\phi;k)U^s_r(\phi;n) + V^s_r(\phi;k)V^s_r(\phi;n) + \left(\frac{\lambda_k}{\lambda_n}\right)^{1/2} Z^s_r(\phi;k)Z^s_r(\phi;n)\Big\} + 2\bar{\alpha}_0(\phi)\sin\phi\{V^s_r(\phi;k)U^s_r(\phi;n) + U^s_r(\phi;k)V^s_r(\phi,n)\} - \frac{d\bar{\alpha}_0(\phi)}{d\phi}\cos\phi V^s_r(\phi;k)U^s_r(\phi;n) + \frac{1}{\gamma}\bar{\alpha}_0(\phi) \times \sin\phi\cos\phi V^s_r(\phi;k)Z^s_r(\phi;n)\frac{\lambda_l}{\sqrt{\lambda_n}}\Bigg]d\mu, \quad \text{(A1)}$$

where $\mu = \cos\phi$,

$$L_{lnk} = \int_{-1}^{1} \Phi_l(\sigma)\Phi_n(\sigma)\Phi_k(\sigma)d\sigma \qquad \text{(A2)}$$

$$Q_n = \int_{-1}^{1} \frac{f(\sigma)}{S(\sigma)} \frac{d\Phi_n}{d\sigma} d\sigma. \qquad \text{(A3)}$$

REFERENCES

Blackmon, M. L., J. E. Geisler and E. J. Pitcher, 1983: A general circulation model study of January climate anomaly patterns associated with interannual variation of equatorial Pacific sea surface temperatures. *J. Atmos. Sci.*, **40,** 1410–1425.

Branstator, G., 1983: Horizontal energy propagation in a barotropic atmosphere with meridional and zonal structure. *J. Atmos. Sci.*, **40,** 1689–1708.

——, 1985: Analysis of general circulation model sea surface temperature anomaly simulations using a linear model. I: Forced solutions. *J. Atmos. Sci.*, **42,** 2225–2241.

Charney, J. G., 1969: A further note on large-scale motions in the tropics. *J. Atmos. Sci.*, **26,** 182–185.

Dickinson, R. E., 1980: Planetary waves: Theory and observation. *Orographic Effects in Planetary Flows,* GARP Publ. Ser. No. 23, Joint Scientific Committee, Geneva, 51–84.

Frederiksen, J. S., 1978: Growth rates and phase speeds of baroclinic waves in multi-level models on a sphere. *J. Atmos. Sci.*, **35,** 1816–1826.

Fulton, S. R., and W. H. Schubert, 1985: Vertical normal mode transforms: Theory and application. *Mon. Wea. Rev.*, **113,** 647–658.

Geisler, J. E., 1981: A linear model of the Walker circulation. *J. Atmos. Sci.*, **38,** 1390–1400.

——, and D. E. Stevens, 1982: On the vertical structure of damped steady circulation in the tropics. *Quart. J. Roy. Meteor. Soc.*, **108,** 87–94.

Gill, A. E., 1980: Some simple solutions for heat-induced tropical circulation. *Quart. J. Roy. Meteor. Soc.*, **106,** 447–462.

Grose, W. L., W. T. Blackshear and R. E. Turner, 1984: The response of a nonlinear, time-dependent, baroclinic model of the atmosphere to tropical thermal forcing. *Quart. J. Roy. Meteor. Soc.*, **110,** 981–1002.

Hendon, H. H., and D. L. Hartmann, 1982: Stationary waves on a sphere: Sensitivity to thermal feedback. *J. Atmos. Sci.*, **39,** 1906–1920.

Holton, J. R., 1971: A diagnostic model for equatorial wave disturbances: The role of vertical shear of the mean zonal wind. *J. Amos. Sci.*, **28,** 55–64.

Horel, J. D., and J. M. Wallace, 1981: Planetary-scale atmospheric phenomena associated with the southern oscillation. *Mon. Wea. Rev.*, **109,** 813–829.

Hoskins, B. J., and D. J. Karoly, 1981: The steady linear response of a spherical atmosphere to thermal and orographic forcing. *J. Atmos. Sci.*, **38,** 1179–1196.

——, A. J. Simmons and D. G. Andrews, 1977: Energy dispersion in a barotropic atmosphere. *Quart. J. Roy. Meteor. Soc.*, **103,** 553–567.

Kasahara, A., 1980: Effect of zonal flows on the free oscillations of a barotropic atmosphere. *J. Atmos. Sci.*, **37,** 917–929.

——, 1984: The linear response of a stratified global atmosphere to tropical thermal forcing. *J. Atmos. Sci.*, **41,** 2217–2237.

Lau, K.-M., and H. Lim, 1982: Thermally driven motions in an equatorial β-plane: Hadley and Walker circulations during the winter season. *Mon. Wea. Rev.*, **110,** 336–353.

Lim, H., and C. P. Chang, 1981: A theory for midlatitude forcing of tropical motions during winter monsoons. *J. Atmos. Sci.*, **38,** 2377–2392.

——, and ——, 1983: Dynamics of teleconnections and Walker circulations forced by equatorial heating. *J. Atmos. Sci.*, **40,** 1897–1915.

——, and ——, 1986: Generation of internal and external mode motions from internal heating: Effects of vertical shear and damping. *J. Atmos. Sci.*, **43,** 948–957.

Matsuno, T., 1966: Quasi-geostrophic motions in the equatorial area. *J. Meteor. Soc. Japan,* **44,** 25–43.

——, 1970: Vertical propagation of stationary planetary waves in the winter Northern Hemisphere. *J. Atmos. Sci.*, **27,** 871–883.

Moura, A. D., and J. Shukla, 1981: On the dynamics of droughts in Northeast Brazil: Observations, theory and numerical experiments with a general circulation model. *J. Atmos. Sci.*, **38,** 2653–2675.

Opsteegh, J. D., and H. M. van den Dool, 1980: Seasonal differences in the stationary response of a linearized primitive equation model: Prospects for long-range forecasting? *J. Atmos. Sci.*, **37,** 2169–2185.

Rosenlof, K. H., D. E. Stevens, J. R. Anderson and P. E. Ciesielski, 1986: The Walker circulation with observed zonal winds, a mean Hadley cell, and cumulus friction. *J. Atmos. Sci.*, **43,** 449–467.

Silva Dias, P. L., W. H. Schubert and M. DeMaria, 1983: Large-scale response of the tropical atmosphere to transient convection. *J. Atmos. Sci.*, **40,** 2689–2707.

Simmons, A. J., 1982: The forcing of stationary wave motion by tropical diabatic heating. *Quart. J. Roy. Meteor. Soc.*, **108,** 503–534.

——, and B. J. Hoskins, 1976: Baroclinic instability on the sphere: Normal modes of the primitive and quasi-geostrophic equations. *J. Atmos. Sci.*, **33,** 1454–1477.

——, J. M. Wallace and G. W. Branstator, 1983: Barotropic wave propagation and instability, and atmospheric teleconnection patterns. *J. Atmos. Sci.*, **40,** 1363–1392.

Tanaka, H., 1985: Global energetics analysis by expansion into three-dimensional normal mode functions during the FGGE winter. *J. Meteor. Soc. Japan,* **63,** 180–200.

Webster, P. J., 1972: Response of the tropical atmosphere to local, steady forcing. *Mon. Wea. Rev.*, **100,** 518–541.

——, 1981: Mechanisms determining the atmospheric response to sea surface temperature anomalies. *J. Atmos. Sci.*, **38,** 554–571.

——, 1982: Seasonality in the local and remote atmospheric response to sea surface temperature anomalies. *J. Atmos. Sci.*, **39,** 41–52.

——, and J. R. Holton, 1982: Cross-equatorial response to middle latitude forcing in a zonally varying basic state. *J. Atmos. Sci.*, **39,** 727–733.